

do not distinguish at this point between path A and path B. Since  $\alpha$ -elimination is, however, well established to be a facile reaction in cationic 16-electron tungstenocene alkyls,<sup>9a,b,c,g</sup> we would propose that path A is the more probable, and this would imply, as speculated previously,<sup>3</sup> that alkene hydride insertion followed by  $\alpha$ -elimination can provide a facile route from alkenes to alkylidenes and may therefore be involved in the initiation of metathesis by some transition-metal catalysts.

**Acknowledgment.** We thank the National Science Foundation and the donors of the Petroleum Research Fund, administered by the American Chemical Society, for their support of this research. We thank Professor D. A. Evans for bringing ref 14 to our attention.

### Isotopic-Label-Directed Observation of the Nuclear Overhauser Effect in Poorly Resolved Proton NMR Spectra

R. H. Griffey, M. A. Jarema, S. Kunz, P. R. Rosevear, and A. G. Redfield\*

Department of Biochemistry, Brandeis University  
Waltham, Massachusetts 02254

Received September 25, 1984

Proton nuclear magnetic resonance spectroscopy (<sup>1</sup>H NMR) is a powerful tool for the determination of structure in chemical and biological systems through observation of the nuclear Overhauser effect (NOE).<sup>1-3</sup> The NOE has a  $r^{-6}$  dependence on internuclear distance and is commonly manifested as a change in population among spatially proximate protons. The NOE can be used to assign <sup>1</sup>H resonances to specific protons in tRNAs and DNA oligomers and to identify local conformation in proteins.<sup>4,5</sup> Unfortunately the lack of resolution in the <sup>1</sup>H NMR spectrum for most large nucleic acids and proteins often precludes unambiguous observation of individual NOEs for overlapping signals.

We describe an extremely simple technique for observing the NOE from a specific proton in a complex spectrum. Incorporation of a stable isotope (<sup>13</sup>C, <sup>15</sup>N) at heteroatomic sites produces a large scalar coupling to a directly bonded proton. Application of on-resonance heteronuclear decoupling collapses the scalar coupling, and the <sup>1</sup>H signal appears as a singlet.<sup>6,7</sup> The usual INDOR experiment uses on- and off-resonance heteronuclear decoupling during acquisition of the <sup>1</sup>H signal to determine heteronuclear chemical shifts. When heteronuclear decoupling and preirradiation at the nominal <sup>1</sup>H frequency are applied simultaneously, the resonance for the proton can be saturated. In contrast, if on-resonance <sup>1</sup>H saturation is applied in the same way but the frequency of the heteronuclear decoupler is displaced, the <sup>1</sup>H signal from the directly bonded proton is not saturated as the frequencies of the signal are shifted by  $\pm J/2$ . The peaks from other protons that have <sup>1</sup>H chemical shifts coincident with the decoupled H-X proton are equally saturated in both cases. Subtraction of the two spectra, with on- and off-resonance heteronuclear decoupling during the period of proton preirradiation, produces a difference

spectrum that displays only the NOE from the proton bonded to the uncommon isotope. The NOE from nearby or overlapping proton lines is canceled in the subtraction.

We first demonstrate the experiment for a small molecule, [1,3-<sup>15</sup>N<sub>2</sub>]uracil. Signals from the two imino protons, at N3 and N1, appear at 11.08 and 10.90 ppm in the 500-MHz spectrum. However, as shown in Figure 1a, the two doublets ( $J_{\text{NH}} = 95$  Hz) overlap. The resonance for the proton at N1 can be assigned because its splitting is decoupled at the expected <sup>15</sup>N chemical shift of 130.6 ppm relative to ammonia for N1, as seen in Figure 1b.<sup>6</sup> The isotopic-label-directed NOE experiment, given in Figure 1c, shows the expected result: the control, with off-resonance <sup>15</sup>N decoupling, produces a doublet while simultaneous on-resonance <sup>15</sup>N and <sup>1</sup>H irradiation saturates the central component (seen in the INDOR experiment of Figure 1b). Subtraction removes the signal from the proton at N3, which is only slightly perturbed by the <sup>15</sup>N rf. Saturation of H1 produces a positive NOE of 4% to the proton at C6, while no NOE is observed to the proton at C5.

In tRNAs, introduction of the <sup>15</sup>N label, on the N3 or N1 of uridine or guanosine, respectively, provides a handle to sort out the poorly resolved proton signals.<sup>7,8</sup> The 500-MHz <sup>1</sup>H spectrum for *E. coli* tRNA<sup>Gm</sup> (Figure 2a) has a composite two-proton signal at 13.8 ppm.<sup>9</sup> Upon preirradiation there are two NOEs, at 7.37 and 8.25 ppm. The NOE at 8.25 ppm disappears in a tRNA sample biosynthetically deuterated at the purine C8 position, showing that it and one of the two 13.8 ppm proton resonances come from one of the two reverse-Hoogsteen base pairs T54A58 or sU8A14.<sup>10,11</sup> Other evidence strongly suggests that it is from T54A58, and this is consistent with the <sup>15</sup>N shifts for the nitrogens to which the 13.8 ppm protons are bonded, which are 163.4 and 160.5 ppm as determined by a 2D forbidden echo experiment.<sup>6,8,11</sup> As shown in Figure 2c, application of <sup>1</sup>H preirradiation combined with <sup>15</sup>N decoupling at these distinct nitrogen frequencies permits the selective observation of the NOE from the two protons. Irradiation at 13.80 and 163.4 ppm produces an NOE at 7.37 ppm. Similar saturation at 13.80 and 160.5 ppm gives rise to an NOE at 8.25 ppm. This triple correlation of nitrogen, imino proton, and ring carbon proton resonances unambiguously assigns the T54 <sup>15</sup>N3 to the 160.5 ppm resonance, consistent with observations in other tRNAs that N3 of T54 in the invariant T54A58 base pair resonates at slightly higher field than the uracil N3 of standard Watson-Crick pairs.<sup>6-8</sup> For future studies it permits shifts of the proton and <sup>15</sup>N resonances of this base pair to be observed separately from those of other overlapping peaks, as a function of solution conditions.

This methodology should be applicable to a variety of chemical and biological problems. As illustrated for *E. coli* tRNA<sup>Gm</sup>, the method would allow the NOE in suitably labeled RNA or DNA to be observed, even in congested regions of the spectrum where the resonances from GC and AU base pairs overlap. A similar advantage may be obtained in large proteins, where aromatic and amide protons both generate peaks between 7 and 9 ppm. Regio-specific incorporation of a <sup>13</sup>C or <sup>15</sup>N isotope will permit the NOE from the C $\alpha$  and amide protons, for example, to be observed for a specific amino acid. Saturation transfer experiments on complex mixtures of labeled compounds could be performed in this way, to elucidate chemical or metabolic rate constants. Finally, the technique is of great value in studies of the interaction of small molecules with large biopolymers. The <sup>1</sup>H chemical shifts for the protons of interest in the small compound usually fall on resonances from protein, and selective saturation of only the protons of the small molecule is not possible. The methodology we describe offers a convenient solution to the problem. We have

(1) Abbreviations used: NOE, nuclear Overhauser effect; tRNA, transfer ribonucleic acid; DNA, deoxyribonucleic acid; rf, radio frequency, 2D, two dimensional.

(2) Roy, S.; Redfield, A. G. *Biochemistry* 1983, 22, 1386-1390.

(3) Noggle, J. H.; Schirmer, R. E. "The Nuclear Overhauser Effect"; Academic Press: New York, 1971.

(4) Schimmel, P. R.; Redfield, A. G. *Annu. Rev. Biophys. Bioeng.* 1980, 9, 181-227.

(5) Jardetzky, G.; Roberts, G. C. K. "NMR in Molecular Biology"; Academic Press: New York, 1981.

(6) Griffey, R. H. Ph.D. Thesis, University of Utah, Salt Lake City, 1984.

(7) Griffey, R. H.; Poulter, C. D.; Yamaizumi, Z.; Nishimura, S.; Hawkins, B. L. *J. Am. Chem. Soc.* 1983, 105, 141-143.

(8) Roy, S.; Papastavros, M. Z.; Sanchez, V.; Redfield, A. G. *Biochemistry* 1984, 23, 4395-4400.

(9) The <sup>15</sup>N label was incorporated by growing a strain of *E. coli* on minimal media containing <sup>15</sup>N ammonium chloride. The tRNA<sup>Gm</sup> was purified on a DE-52 column at pH 7.5 and a DEAE-Sephadex column at pH 7.5.

(10) Sanchez, V.; Redfield, A. G.; Johnston, P. D.; Tropp, J. *Proc. Natl. Acad. Sci. U.S.A.* 1981, 77, 5959-5962.

(11) Jarema, M.; Redfield, A. G., unpublished results.

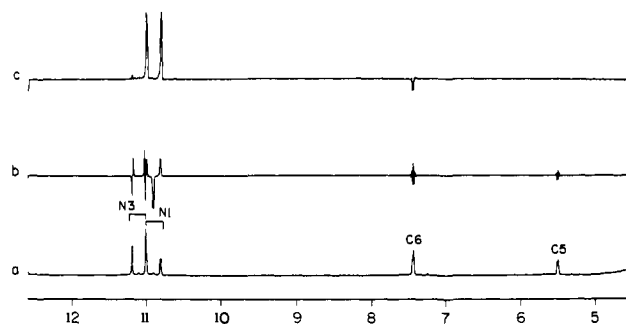


**Figure 1.** Isotopic-label-directed NOE experiment on 50 mM  $[1,3-^{15}\text{N}_2]$ uracil in dimethyl sulfoxide. (a) A control proton NMR experiment with no heteronuclear irradiation; the signals at 7.44 and 5.49 ppm are from the unlabeled protons at C6 and C5, respectively. (b) A  $^1\text{H}$ - $^{15}\text{N}$  INDOOR experiment; in contrast to (c), there is no proton preirradiation, and strong  $^{15}\text{N}$  decoupling is applied on and off resonance during the free induction decay. Residual features at C5H and C6H come from the small coupling between these protons and  $^{15}\text{N}1$ . (c) The isotopic-label-directed experiment for the proton at N1; a total of 320 scans were acquired with alternate on- and off-resonance  $^{15}\text{N}$  preirradiation combined with  $^1\text{H}$  preirradiation at 10.90 ppm for 1 s.

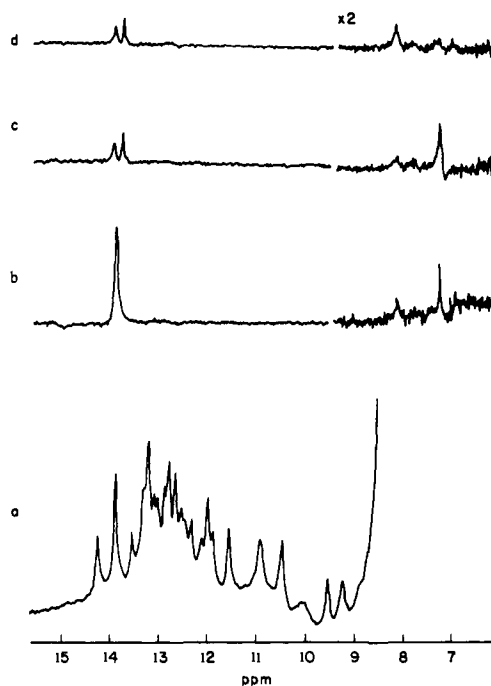


**Figure 2.** Isotopic-label-directed NOE experiment with *E. coli* tRNA<sup>Gln</sup>. (a) A control spectrum of unlabeled tRNA<sup>Gln</sup> at 20 °C. (b) Preirradiation of the peak at 13.88 ppm for 100 ms. (c)  $^1\text{H}$  preirradiation of  $^{15}\text{N}$ -enriched tRNA<sup>Gln</sup> at 13.88 ppm with  $^{15}\text{N}$  preirradiation on resonance at 163.2 ppm. (d)  $^1\text{H}$  preirradiation at 13.88 ppm with  $^{15}\text{N}$  preirradiation on resonance at 160.4 ppm. A total of 2000 scans were acquired with on- and off-resonance  $^{15}\text{N}$  preirradiation. Both tRNA samples were dissolved in a 10 mM sodium phosphate buffer containing 100 mM sodium chloride, 10 mM magnesium chloride, 1 mM sodium thiosulfate, and 5% deuterium oxide.

demonstrated the method for  $^{15}\text{N}$ -enriched molecules, but it will prove of equal benefit with  $^{13}\text{C}$ -labeled compounds, where the one-bond scalar coupling is 140–200 Hz.

**Acknowledgment.** This research was supported by U.S.P.H.S. Grant GM20168. R.H.G. was supported by NIH Public Health Service Fellowship GM09700. The *E. coli* strain was constructed by Robert Swanson and kindly provided by Prof. D. Soll of Yale University. This is contribution number 1542 from the Brandeis University Biochemistry Department.

**Registry No.**  $[1,3-^{15}\text{N}_2]$ Uracil, 5522-55-4.

## Syntheses and X-ray Structures of $[\text{Li}(\text{THF})_4][\text{Ni}(\text{NPh}_2)_3] \cdot 0.5\text{C}_7\text{H}_8$ , $[\text{Ni}(\text{NPh}_2)_2]_2$ , and $[\text{Co}(\text{NPh}_2)_2]_2$ : Structural Characterization of Three Coordinate First-Row $d^7$ and $d^8$ Complexes

Håkon Hope, Marilyn M. Olmstead, Brendan D. Murray, and Philip P. Power\*

Department of Chemistry, University of California Davis, California 95616  
Received October 9, 1984

The synthesis of  $\text{Ti}(\text{NPh}_2)_4$ , the first transition-metal amide, was reported in 1935.<sup>1</sup> However, it was only recently that Fröhlich et al. extended the application of the interesting diphenylamido group to other d-block elements.<sup>2-5</sup> In the interim, other transition-metal amides, especially complexes of the  $\text{NMe}_2$  and  $\text{N}(\text{SiMe}_3)_2$  groups, have been intensively investigated.<sup>6-8</sup> These studies suggest that, apart from a few  $\text{N}(\text{SiMe}_3)_2$  derivatives, it is difficult to prepare stable homoleptic<sup>9</sup> amido complexes of the later ( $\text{Fe} \rightarrow \text{Cu}$ ) transition metals. The sole, structurally characterized, exceptions are the closed-shell complex  $[(\text{CuNET}_2)_4]^{10}$  and  $[\text{Co}(\text{NPh}_2)_2]_2$ , which was reported to have a unique unsupported Co-Co bond.<sup>3</sup> In this paper we will show that the cobalt complex exists rather as an amido-bridged dimer. Here we also report the first structures of two homoleptic diaryl amides of Ni(II) which have a first-row  $d^8$  metal in the unreported trigonal-planar geometry.

The nickel complexes  $[\text{Li}(\text{THF})_4][\text{Ni}(\text{NPh}_2)_3] \cdot 0.5\text{PhMe}$  (**1**) and  $[\text{Ni}(\text{NPh}_2)_2]_2$  (**2**) were synthesized by treating a  $-78^\circ\text{C}$  THF slurry of anhydrous  $\text{NiCl}_2$  with 2 equiv of a THF/hexane solution of  $\text{LiNPh}_2$ . The reaction mixture became navy blue on warming to  $25^\circ\text{C}$  and was stirred for an additional 2 h. The volatiles were removed in vacuo and the residue redissolved in hot toluene, filtered, and cooled to give ca. 50% yield of **2** as dark green crystals. Alternatively a mixture comprised of equal volumes of ether/hexane/toluene may be added to the original blue reaction mixture. Filtration followed by slow cooling to  $-20^\circ\text{C}$  gave **1**, as navy blue crystals in 40% yield.<sup>11</sup> Substitution of  $\text{CoCl}_2$  for  $\text{NiCl}_2$  under similar conditions yielded a green complex which analyzed as  $[\text{Li}(\text{THF})_4][\text{Co}(\text{NPh}_2)_3] \cdot 0.5\text{PhMe}$  (**3**) (25% yield) and the brown-red complex  $[\text{Co}(\text{NPh}_2)_2]_2$  (**4**) in 45% yield.<sup>12</sup>

The structures of **1**, **2**, and **4** were determined by X-ray diffraction<sup>13</sup> and are illustrated in Figures 1 (anion only) and 2. The structure of  $[\text{Ni}(\text{NPh}_2)_3]^-$  consists of a roughly trigonal-planar  $\text{NiN}_3$  array with an approximate  $D_{3h}$  field at the metal leading to two unpaired electrons in the  $e'$  orbitals. This is supported by a  $\mu$  at 298 K of  $2.6 \mu_B$ . The average Ni-N distance of 1.89 Å is close to that expected from published covalent radii.<sup>14</sup> The

- (1) Dermer, O. C.; Fernelius, W. C. *Z. Anorg. Allg. Chem.* **1935**, *221*, 83.
- (2) Fröhlich, H. O.; Märkisch, V. *Z. Chem.* **1975**, *15*, 276.
- (3) Brito, V.; Fröhlich, H. O.; Müller, B. *Z. Chem.* **1979**, *19*, 28.
- (4) Fröhlich, H. O.; Römhild, W. *Z. Chem.* **1979**, *19*, 414.
- (5) Fröhlich, H. O.; Römhild, W. *Z. Chem.* **1980**, *20*, 154.
- (6) Bradley, D. C.; Chisholm, M. H. *Acc. Chem. Res.* **1976**, *9*, 273.
- (7) Harris, D. M.; Lappert, M. F. *J. Organomet. Chem. Libr.* **1976**, *2*, 13.
- (8) Bradley, D. C. *Chem. Br.* **1975**, *11*, 393.
- (9) Murray, B. D.; Power, P. P. *Inorg. Chem.* **1984**, *26*, 4584.
- (10) Lappert, M. F.; Power, P. P.; Sanger, A. R.; Srivastava, R. C. "Metal and Metalloid Amides"; Ellis Horwood: Chichester, England, 1980.
- (11) Davidson, P. J.; Lappert, M. F.; Pearce, R. *Acc. Chem. Res.* **1974**, *7*, 209.
- (12) Hope, H.; Power, P. P. *Inorg. Chem.* **1984**, *23*, 936.
- (13) Anal. Calcd for **1**: C, 73.68; H, 7.35; N, 4.64. Found: C, 74.2; H, 7.73; N, 4.4. Mp  $115^\circ\text{C}$ . Anal. Calcd for **2**: C, 72.95; H, 5.10; N, 7.09. Found: C, 72.8; H, 5.1; N, 7.0. Mp  $140^\circ\text{C}$ .
- (14) Anal. Calcd for **3**: C, 73.66; H, 7.35; N, 4.64. Found: C, 74.1; H, 7.4; N, 4.4. Mp  $138^\circ\text{C}$ . Anal. Calcd for **4**: C, 72.91; H, 5.10; N, 7.09. Found: C, 72.8; H, 5.1; N, 6.9.
- (15) Crystal data:  $[\text{Li}(\text{THF})_4][\text{Ni}(\text{NPh}_2)_3] \cdot 0.5\text{C}_7\text{H}_8$  (**1**)  $P\bar{1}$ ,  $T = 140\text{ K}$ ,  $a = 9.948$  (2) Å,  $b = 13.640$  (2) Å,  $c = 18.237$  (3) Å,  $\alpha = 95.84$  (1)°,  $\beta = 92.83$  (2)°,  $\gamma = 102.10$  (1)°,  $R = 0.044$  for 698 parameters, 4289 unique observed reflections;  $[\text{Ni}(\text{NPh}_2)_2]_2$  (**2**)  $Pc$ ,  $T = 140\text{ K}$ ,  $a = 9.372$  (2) Å,  $b = 10.122$  (2) Å,  $c = 20.648$  (4) Å,  $\beta = 102.31$  (2)°,  $R = 0.060$  for 245 parameters, 2185 unique observed reflections;  $[\text{Co}(\text{NPh}_2)_2]_2$  (**4**)  $P2_1/n$ ,  $T = 140\text{ K}$ ,  $a = 9.040$  (3) Å,  $b = 21.351$  (7) Å,  $c = 9.927$  (3) Å,  $\beta = 95.62$  (3)°,  $R = 0.067$  for 125 parameters, 1221 unique observed reflections.